Expression, purification and crystallization of the Atg5–Atg16 complex essential for autophagy

Minako Matsushita,[a] Nobuo N. Suzuki,[a] Yuko Fujioka,[a] Yoshinori Ohsumi[b] and Fuyuhiko Inagaki[a]*

[a]Department of Structural Biology, Graduate School of Pharmaceutical Sciences, Hokkaido University, N-12, W-6, Kita-ku, Sapporo 060-0812, Japan, and [b]Department of Cell Biology, National Institute for Basic Biology, 38 Nishigonaka, Myodaiji, Okazaki 444-8585, Japan

Correspondence e-mail: finagaki@pharm.hokudai.ac.jp

Atg5 is a novel 34 kDa protein that is covalently modified by Atg12, a ubiquitin-like modifier, and forms a complex with Atg16. The Atg12–Atg5–Atg16 complex localizes to autophagosome precursors and plays an essential role in autophagosome formation. *Saccharomyces cerevisiae* Atg5 in complex with the N-terminal regions of Atg16 was expressed, purified and crystallized in four crystal forms. Forms I, II and III belong to space group $P2_1$, with unit-cell parameters $a = 66.3$, $b = 104.4$, $c = 112.1$ Å, $\beta = 92.1°$ (form I), $a = 79.5$, $b = 101.4$, $c = 95.1$ Å, $\beta = 98.6°$ (form II) or $a = 56.9$, $b = 101.2$, $c = 66.5$ Å, $\beta = 100.6°$ (form III). Form IV belongs to space group $P4_22_12$, with unit-cell parameters $a = 73.3$, $c = 148.1$ Å. Diffraction data were collected from all crystal forms and high-resolution data to beyond 2.0 Å resolution were obtained from a form IV crystal.

1. Introduction

Autophagy is a starvation-induced response that mediates the bulk degradation of cytoplasmic components in lysosomes/vacuoles (Seglen & Bohley, 1992; Takeshige *et al.*, 1992) and plays a critical role in numerous biological processes such as neurodegeneration and pathogen infection as well as survival response during neonatal starvation (Hara *et al.*, 2006; Komatsu *et al.*, 2006; Ogawa *et al.*, 2005; Nakagawa *et al.*, 2004; Kuma *et al.*, 2004). In autophagy, a double-membrane structure called an autophagosome sequesters a portion of cytoplasm and fuses with the lysosome/vacuole to deliver its contents into the organelle lumen.

16 autophagy genes involved in autophagosome formation, named *ATG* genes, have been identified using genetic approaches in *Saccharomyces cerevisiae* (Klionsky *et al.*, 2003). Among these, five Atg proteins were shown to be involved in a novel ubiquitin-like conjugation system named the Atg12 system (Mizushima *et al.*, 1998). In the Atg12 system, the carboxyl-terminal glycine of Atg12 is activated by Atg7, an E1-like enzyme (Tanida *et al.*, 1999), and is then transferred to Atg10, an E2-like enzyme (Shintani *et al.*, 1999). Finally, Atg12 is conjugated to its sole target, Atg5 (Mizushima *et al.*, 1998). In addition to the covalent interaction with Atg12, Atg5 interacts with the N-terminal region of a multimeric protein, Atg16, non-covalently (Mizushima *et al.*, 1999). Using this interaction, the Atg12–Atg5 conjugate forms a multimeric complex with Atg16 (Kuma *et al.*, 2002; Mizushima *et al.*, 1999). The Atg12–Atg5–Atg16 complex localizes to autophagosome precursors and plays an essential role in autophagosome formation (Kim *et al.*, 2001; Suzuki *et al.*, 2001).

Recently, we reported the crystal structure of plant Atg12 and revealed that Atg12 is a ubiquitin-fold protein (Suzuki *et al.*, 2005). However, structural information on Atg5 and Atg16 is completely lacking, preventing us from elucidating the molecular role of the Atg12–Atg5–Atg16 complex. In this report, we describe the expression, purification and crystallization of Atg5 in complex with the N-terminal region of Atg16.

2. Expression and purification

The full-length gene of *S. cerevisiae* Atg5 was inserted into a pHT1 vector [a pET28a(+) vector (Novagen) modified by insertion of

1021
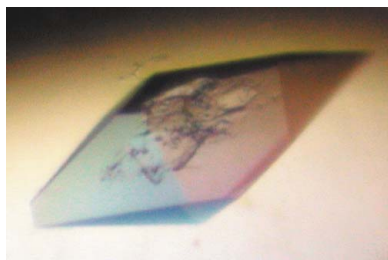
sequences encoding a hexahistidine tag and a TEV protease-cleavage site] using *Nde*I/*Bam*HI restriction sites. Residues 1–46 and 1–57 of *S. cerevisiae* Atg16 were inserted into a pET-11a vector (Novagen) using *Nde*I/*Bam*HI restriction sites. Each Atg16 construct was co-expressed with N-terminally hexahistidine-tagged Atg5 in *Escherichia coli* BL21 (DE3). After cell lysis, Atg5 was purified by affinity chromatography using an Ni–NTA column (Qiagen). Throughout the purification steps, both Atg16(1–46) and Atg16(1–57) co-migrated with Atg5, indicating that they form a stable complex with Atg5. After affinity chromatography, the protein complexes were purified on a HiTrap DEAE FF column (GE Healthcare Biosciences) equilibrated with 20 m*M* Tris–HCl pH 8.5 and were eluted with a 0–500 m*M* NaCl gradient in the same buffer. The hexahistidine tag was then cleaved from Atg5 with TEV protease (GE Healthcare Biosciences; a Gly-Ala-His sequence remained on the N-terminus of Atg5). Further purification was performed using a HiTrap CM FF column (GE Healthcare Biosciences) equilibrated with 20 m*M* HEPES buffer pH 6.8 and product was eluted with a 0–500 m*M* NaCl gradient in the same buffer. Final purification was carried out on a Superdex75 column (GE Healthcare Biosciences) eluted with 20 m*M* HEPES buffer pH 6.8 and 150 m*M* NaCl for the Atg5–Atg16(1–46) complex and on a Superdex200 column (GE Healthcare Biosciences) eluted with 20 m*M* Tris buffer pH 7.4 and 150 m*M* NaCl for the Atg5–Atg16(1–57) complex. The purified Atg5–Atg16(1–46) and Atg5–Atg16(1–57) complexes (Fig. 1) were concentrated to 8 and 12.5 mg ml^{-1}, respectively, and used for crystallization.

3. Crystallization

Crystallization trials were performed using the sitting-drop vapour-diffusion method at 293 K. Initial screening was performed using Crysta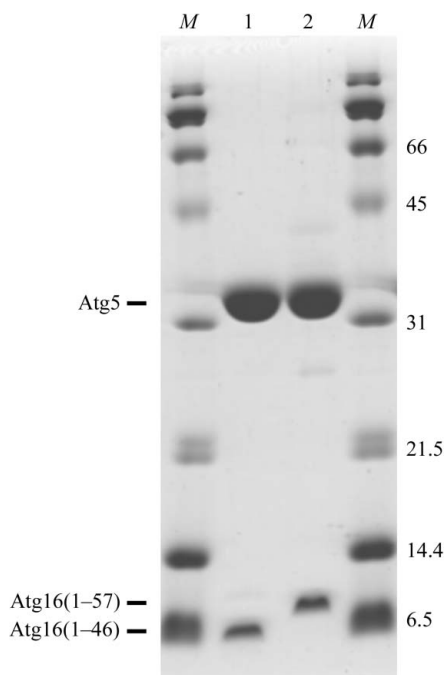l Screen and Crystal Screen 2 from Hampton Research and Wizard I and II from Emerald Biostructures as reservoir solutions. 0.3 µl drops of 8 mg ml^{-1} Atg5–Atg16(1–46) complex in 20 m*M* HEPES buffer pH 6.8 and 150 m*M* NaCl were mixed with equal amounts of reservoir solution and were equilibrated against 100 µl of the same reservoir solution by vapour diffusion. In the same way, 0.3 µl drops of 12.5 mg ml^{-1} Atg5–Atg16(1–57) complex in 20 m*M* Tris buffer pH 7.4 and 150 m*M* NaCl were mixed with equal amounts of reservoir solution and were equilibrated against 100 µl of the same reservoir solution by vapour diffusion. The Atg5–Atg16(1–46) complex was crystallized with a reservoir solution consisting of 24% PEG 3350, 0.1 *M* CAPS pH 10.0 (form I crystal). The Atg5–Atg16(1–57) complex was crystallized in three different crystal forms (forms II, III and IV). Only a photograph of form IV is shown in Fig. 2, as we judge the photographs we have of the other forms to not be good enough for publication. These three crystal forms were obtained with the same reservoir solution consisting of 15% PEG 3350, 0.1 *M* HEPES pH 6.8. All crystals were obtained within a week.

4. Preliminary X-ray analysis

Crystals were immersed into reservoir solution supplemented with 11–20% glycerol as a cryoprotectant for several seconds and then flash-cooled and kept in a stream of nitrogen gas at 90–120 K during data collection. Diffraction data were collected from a form I crystal using an ADSC Quantum 315 charge-coupled device detector on SPring-8 beamline BL41XU at a wavelength of 1.00 Å. Diffraction data from form II, III and IV crystals were collected on a Rigaku R-AXIS VII imaging-plate detector using Cu *K*α radiation. All diffraction data were processed using the *HKL*-2000 program suite (Otwinowski & Minor, 1997). The data-collection statistics are summarized in Table 1. The acceptable range of the volume-to-weight ratio (V_M) values (Matthews, 1968) indicates that form I contains three, four or five Atg5–Atg16(1–46) complexes (the corresponding V_M values are 3.31, 2.48 and 1.99 Å^3 Da^{-1}, respectively), form II contains three, four or five Atg5–Atg16(1–57) complexes (V_M values of 3.15, 2.36 and 1.89 Å^3 Da^{-1}, respectively), form III contains two Atg5–Atg16(1–57) complexes (V_M = 2.35 Å^3 Da^{-1}) and form IV contains one Atg5–Atg16(1–57) complex (V_M = 2.48 Å^3 Da^{-1}) per asymmetric unit. We calculated self-rotation functions using form I and II diffraction data, but failed to find any obvious noncrystallo-
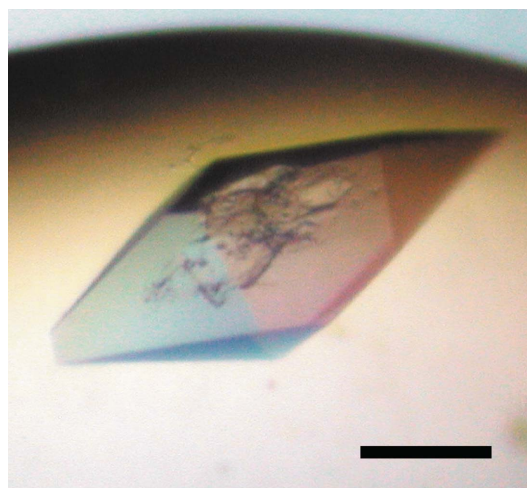

Figure 1
SDS–PAGE of purified Atg5–Atg16(1–46) and Atg5–Atg16(1–57) complexes on a 15% gel. Lanes 1 and 2 contain Atg5–Atg16(1–46) and Atg5–Atg16(1–57) complexes, respectively, and lanes *M* contain molecular-weight markers (labelled in kDa). Proteins were stained with Coomassie Brilliant Blue.

Figure 2
Crystal of Atg5–Atg16(1–57) complex (form IV). The black scale bar is 100 µm in length.

Table 1
Diffraction data statistics of four crystal forms of the Atg5–Atg16 complex.

Values in parentheses refer to the outer shell.

Crystal form	I	II	III	IV
Protein complex	Atg5–Atg16(1–46)	Atg5–Atg16(1–57)	Atg5–Atg16(1–57)	Atg5–Atg16(1–57)
Space group	$P2_1$	$P2_1$	$P2_1$	$P4_22_12$
Unit-cell parameters				
$\quad a$ (Å)	66.3	79.5	56.9	73.3
$\quad b$ (Å)	104.4	101.4	101.2	73.3
$\quad c$ (Å)	112.2	95.1	66.5	148.1
$\quad \beta$ (°)	92.1	98.6	100.6	90
Resolution range (Å)	50–2.1 (2.18–2.10)	50–2.95 (3.06–2.95)	50–3.0 (3.11–3.00)	50–1.97 (2.04–1.97)
Observed reflections	317606	169957	74216	257319
Unique reflections	88015	31125	14118	29390
Completeness (%)	98.6 (95.7)	98.8 (91.5)	94.3 (77.8)	99.9 (100.0)
$R_{\mathrm{merge}}(I)$†	0.048 (0.306)	0.092 (0.312)	0.090 (0.304)	0.055 (0.304)
$I/\sigma(I)$	15.0 (3.8)	8.7 (3.9)	10.9 (4.0)	28.9 (11.1)

† $R_{\mathrm{merge}}(I) = (\sum \sum |I_i - \langle I \rangle|)/\sum \sum I_i$, where I_i is the intensity of the ith observation and $\langle I \rangle$ is the mean intensity.

graphic symmetry axes. Therefore, the numbers of complexes contained in the asymmetric units of form I and II crystals remain to be determined. Phasing experiments are now in progress by a combination of the multiple isomorphous replacement and multi-wavelength anomalous dispersion methods.

References

Hara, T., Nakamura, K., Matsui, M., Yamamoto, A., Nakahara, Y., Suzuki-Migishima, R., Yokoyama, M., Mishima, K., Saito, I., Okano, H. & Mizushima, N. (2006). *Nature (London)*, **441**, 885–889.

Kim, J., Huang, W. P. & Klionsky, D. J. (2001). *J. Cell Biol.* **152**, 51–64.

Klionsky, D. J., Cregg, J. M., Dunn, W. A. Jr, Emr, S. D., Sakai, Y., Sandoval, I. V., Sibirny, A., Subramani, S., Thumm, M., Veenhuis, M. & Ohsumi, Y. (2003). *Dev. Cell*, **5**, 539–545.

Komatsu, M., Waguri, S., Chiba, T., Murata, S., Iwata, J., Tanida, I., Ueno, T., Koike, M., Uchiyama, Y., Kominami, E. & Tanaka, K. (2006). *Nature (London)*, **441**, 880–884.

Kuma, A., Hatano, M., Matsui, M., Yamamoto, A., Nakaya, H., Yoshimori, T., Ohsumi, Y., Tokuhisa, T. & Mizushima, N. (2004). *Nature (London)*, **432**, 1032–1036.

Kuma, A., Mizushima, N., Ishihara, N. & Ohsumi, Y. (2002). *J. Biol. Chem.* **277**, 18619–18625.

Matthews, B. W. (1968). *J. Mol. Biol.* **33**, 491–497.

Mizushima, N., Noda, T. & Ohsumi, Y. (1999). *EMBO J.* **18**, 3888–3896.

Mizushima, N., Noda, T., Yoshimori, T., Tanaka, Y., Ishii, T., George, M. D., Klionsky, D. J., Ohsumi, M. & Ohsumi, Y. (1998). *Nature (London)*, **395**, 395–398.

Nakagawa, I., Amano, A., Mizushima, N., Yamamoto, A., Yamaguchi, H., Kamimoto, T., Nara, A., Funao, J., Nakata, M., Tsuda, K., Hamada, S. & Yoshimori, T. (2004). *Science*, **306**, 1037–1040.

Ogawa, M., Yoshimori, T., Suzuki, T., Sagara, H., Mizushima, N. & Sasakawa, C. (2005). *Science*, **307**, 727–731.

Otwinowski, Z. & Minor, W. (1997). *Methods Enzymol.* **276**, 307–326.

Seglen, P. O. & Bohley, P. (1992). *Experientia*, **48**, 158–172.

Shintani, T., Mizushima, N., Ogawa, Y., Matsuura, A., Noda, T. & Ohsumi, Y. (1999). *EMBO J.* **18**, 5234–5241.

Suzuki, K., Kirisako, T., Kamada, Y., Mizushima, N., Noda, T. & Ohsumi, Y. (2001). *EMBO J.* **20**, 5971–5981.

Suzuki, N. N., Yoshimoto, K., Fujioka, Y., Ohsumi, Y. & Inagaki, F. (2005). *Autophagy*, **1**, 119–126.

Takeshige, K., Baba, M., Tsuboi, S., Noda, T. & Ohsumi, Y. (1992). *J. Cell Biol.* **119**, 301–311.

Tanida, I., Mizushima, N., Kiyooka, M., Ohsumi, M., Ueno, T., Ohsumi, Y. & Kominami, E. (1999). *Mol. Biol. Cell*, **10**, 1367–1379.